Published in final edited form as:
Neuroscience. 2014 January 31; 258: 174–183. doi:10.1016/j.neuroscience.2013.11.003.

Adolescent social isolation enhances the plasmalemmal density of NMDA NR1 subunits in dendritic spines of principal neurons in the basolateral amygdala of adult mice

Jerylin O. Gan[1], **Everett Bowline**[1], **Frederico S. Lourenco**[2], and **Virginia M. Pickel**[1]

Jerylin O. Gan: jog2032@med.cornell.edu

[1]Brain and Mind Research Institute, Weill Cornell Medical College, New York, New York, 10065

[2]Sackler Institute for Developmental Psychobiology, Weill Cornell Medical College, New York, NY 10065, USA

Abstract

Social isolation during the vulnerable period of adolescence produces emotional dysregulation manifested by abnormalities in adult behaviors that require emotional processing. The affected brain regions may include the basolateral amygdala (BLA), where plasticity of glutamatergic synapses in principal neurons plays a role in conditioned emotional responses. This plasticity is dependent on NMDA receptor trafficking denoted by intracellular mobilization of the obligatory NR1 NMDA subunit. We tested the hypothesis that the psychosocial stress of adolescent social isolation (ASI) produces a lasting change in NMDA receptor distribution in principal neurons in the BLA of adults that express maladaptive emotional responses to sensory cues. For this, we used behavioral testing and dual electron microscopic immunolabeling of NR1 and CaMKII, a protein predominantly expressed in principal neurons of the BLA in adult C57Bl/6 mice housed in isolation or in social groups from post-weaning day 22 until adulthood (~3 months of age). The isolates showed persistent deficits in sensorimotor gating evidenced by altered prepulse inhibition (PPI) of acoustic startle and hyperlocomotor activity in a novel environment. Immunogold-silver labeling for NR1 alone or together with CaMKII was seen in many somatodendritic profiles in the BLA of all mice irrespective of rearing conditions. However, isolates compared with group-reared mice had a significantly lower cytoplasmic (4.72±0.517 vs 6.31 ± 0.517) and higher plasmalemmal (0.397±0.0779 vs 0.216±0.026) density of NR1 immunogold particles in CaMKII-containing dendritic spines. There were no rearing-dependent difference is the size or number of these spines or those of other dendritic profiles within the neuropil, which also failed to show an impact of ASI on NR1 immunogold labeling. These results provide the first evidence that ASI enhances the surface trafficking of NMDA receptors in dendritic spines of principal neurons in the BLA of adult mice showing maladaptive behaviors that are consistent with emotional dysregulation.

Address correspondence to: Dr. Virginia M. Pickel, Brain and Mind Research Institute, 407 East 61st Street New York, NY 10065, Phone: (646) 962-8275, Fax: (646) 962-0535, vpickel@med.cornell.edu.

Keywords

schizophrenia; prepulse inhibition; hyperlocomotor activity; glutamate; electron microscopic immunolabeling; CaMKII

Introduction

Animal models and human imaging studies suggest that disturbances in the basolateral amygdala (BLA) play a role in the emotional dysregulation characteristic of many mental health disorders including schizophrenia and bipolar disorder (e.g. dysregulation categorized in the negative valence systems and systems for social process in the Research Domain Criteria classification (Insel et al., 2010). Such dysregulation, loosely defined as an inability to properly process emotionally-charged stimuli, often first manifests during the critical neurodevelopmental period of adolescence, when the prefrontal cortex and other brain regions providing glutamatergic inputs to the BLA continue to develop and mature (Cunningham et al., 2002). The critical involvement of the lateral amygdaloid complex in emotional processing (LeDoux 2000) suggests that improper development of these glutamatergic inputs and ensuing adaptations in BLA output neurons during adolescence may thus contribute to emotional dysregulation seen in mental health disorders (Einon and Morgan, 1977; Lukkes et al., 2012).

BLA projection neurons are pyramidal-like glutamatergic principal neurons that comprise 85% of the neuronal population in this region, distinguishable from interneurons by their content of calcium calmodulin dependent protein kinase II (CaMKII; McDonald, 1992). Ontogenetic studies specifically implicate activity of BLA principal neurons in the mediation of anxiety-related behaviors (Tye et al., 2011). This is consistent with evidence that severe ablations of the BLA lead to the loss of fear response in both animal models and schizophrenics (Bechara et al., 1999). However, more subtly, increased neuronal activity in the BLA can result in decreased social interaction and altered responses to novel stimuli (Benes, 2009; Stuber et al., 2011). Moreover, pharmacological manipulation of glutamate and dopamine in the BLA alters prepulse inhibition (PPI) to acoustic startle response (Bakshi and Geyer, 1998; Stevenson and Gratton, 2004). PPI, a phenomenon in which involuntary reactions to a startling stimulus is decreased by a preceding non-startling stimulus, is a measure of sensorimotor gating. Deficits in PPI are thought to indicate the inability of schizophrenics to filter environmental stimuli, leading to cognitive overload and emotional dysregulation (Geyer and Moghaddam, 2002). Sensorimotor gating deficits also manifests in rodents as sustained hyperlocomotion in a novel environment due to an inability to habituate to novel stimuli (Levine et al., 2007). Stress during adolescence, such as post-weaning adolescent social isolation (ASI), in which rodents are housed individually from weaning until adulthood, alters animal behavior similarly to direct BLA disruption (Geyer and Moghaddam, 2002; Lukkes, 2009). As a result of this stressful early-life experience, rodents display irreversible abnormalities in their responses to novel environments and have deficits in PPI (Braff and Geyer, 1990).

The processing of emotional information in these complex behaviors may be susceptible to disruption through improper ontogenetic development of NMDA receptor populations on principal neurons in the BLA (Benes, 2009). NMDA receptors are often required for activity-dependent plasticity of glutamatergic synapses (Wenthold et al., 2003). These receptors, which are comprised of NR1 subunits or a combination of an obligatory NR1 and various NR2 subunits, undergo ontogenetic changes in subunit composition making them more activity-dependent (Barria and Malinow, 2002; 2005). The NR2B expression may make these receptors more susceptible to isolation rearing induced diminution in the sensory

signaling that is essential for social recognition memory (Jacobs and Tsien, 2012). Abnormal NMDA signaling and plasticity is highly implicated in the neuropathology of schizophrenia (Belforte et al., 2009; Adell et al., 2012;). Specifically, postmortem analysis has shown abnormal trafficking of selective isoforms of NR1- and NR1/NR2-containing NMDA receptors in the prefrontal cortex of schizophrenics (Pérez-Otano and Ehlers, 2005; Kristiansen et al., 2010; Rubio et al., 2013). Impaired receptor trafficking can affect neuronal activity by changing receptor availability, possibly contributing to the underlying neuropathology (Radley et al., 2007). It is unknown, however, whether the same trafficking abnormalities are present in the BLA, or whether impairments are caused by environmental/developmental factors.

In this study, we sought to determine whether adolescent isolation resulting in emotional dysregulation produces abnormalities in the surface/synaptic distribution of the requisite NMDA NR1 subunit in CaMKII-containing principal neurons of the adult BLA. For this we used behavioral testing and electron microscopic immunolabeling of the BLA in C57Bl/6 mice reared in isolation or in small groups from weaning to adulthood.

Methods

Animals

The animal protocols in this study were approved by the Animal Care Committee at Weill Medical College of Cornell University and strictly adhere to NIH guidelines concerning the Care and Use of Laboratory Animals in Research. C57/BL6 mice were obtained from Jackson Laboratories (Bar Harbor, Main) immediately after weaning at postnatal day 20). These mice were housed under a 12-hour light/dark cycle with food and water available *ad libitum*.

Adolescent Social Isolation

At post-natal day 21–22, littermate pups were housed either individually or in groups of 3–5 mice per cage. Two nestlet squares were provided in each cage for nesting. While isolated animals could hear and smell other animals within the housing facility, there was no physical interaction with other mice and minimal investigator handling during weekly cage changes (Pietropaolo et al., 2008). Animals were isolated for 8 weeks before initiation of any experimental procedure. All testing was performed on adult animals (~3 months of age).

Acoustic startle response

Adult (~3 months of age) mice that were either group-housed or socially isolated through adolescence were behaviorally tested for sensorimotor gating deficiencies. The startle reflex was recorded using the SR-Lab System (San Diego Instruments; San Diego, CA, USA), with a CAL 002741 startle chamber (Plexiglas cylinder, 12.8 cm long with a 3.3 cm internal diameter) mounted on a platform (12.8 cm × 20.3 cm) in a sound-attenuated cabinet (38.1 cm × 40.6 cm × 58.4 cm). A high-frequency speaker produced both ambient background noise (65 dB) and acoustic stimuli. House lights and an air-circulating fan (75dB) were on for the duration of the testing. The vibrations of the cylinder, produced by whole-body movement of the mouse, were converted to a digital signal by a piezo-electric accelerometer unit attached to the platform and recorded via an analog to digital relay.

The acoustic startle trials consisted of an initial 5-minute period during which the animal was acclimated to a 75 dB background noise, followed by 30 acoustic startle trials. Each trial consisted of a 40 ms acoustic startle pulse (startle, 120 dB) with an average inter-trial interval (ITI) of 15s (range=10–20s). 78, 81, or 87 dB pre-pulses that were 20ms in duration preceded the pulse by 100 ms in pseudorandom trials. The maximum (V_{max}) and average

(V_{ave}) startle response to each stimulus were recorded in standardized units (Hara & Pickel, 2005). All other behavioral testing were performed at least a week after PPI testing to minimize the effects of stress from acoustic startle response testing.

Open field test

Mice were placed in a novel open arena (40 cm × 40 cm × 37 cm) monitored by infrared beams (Med-Associates). Mice were allowed to explore freely for one hour while ambulatory behavior was recorded. Total distance travelled was evaluated for animals that were group- or isolation-housed.

Dual immunoperoxidase and immunogold labeling for electron microscopy

In addition to mice used exclusively for behavioral testing, separate cohort of group (n=5) and isolation (n=4) reared adult mice were processed for electron microscopy. In these animals, we allowed 1–2 week recovery from PPI testing before processing the brain tissue for electron microscopic immunolabeling to minimize the effects of acute stress from behavioral testing. For this, the mice were overdosed with sodium pentobarbital (150 mg/kg, i.p.) and then perfused through the heart with a solution containing 3.75% acrolein/2% paraformaldehyde in 0.1 M phosphate buffer (PB; pH 7.4) followed by 2% paraformaldehyde in PB. Brains were post-fixed in 2% paraformaldehyde in PB for 30 min, removed, then cut on a vibratome into 30 micron thick coronal sections, and stored in cryoprotective solution at −20°C. BLA containing tissue sections (1.94 mm anterior to Bregma; Paxinos and Franklin, 2003) were then processed for dual immunocytochemical labeling. For this, the tissue sections were first incubated for 24 hours at room temperature followed by 24 hours at 4°C in a Tris-buffered saline (TBS) solution containing 0.1% bovine serum albumin and a cocktail of both primary antibodies. These included a polyclonal goat antibody (1:1000) against the α isoform of Ca2+/calmodulin-dependent protein kinase II (CaMKII; Abcam, ab87597, Cambridge, MA) and a monoclonal mouse antibody (1:50) against the NR1 subunit of the NMDA receptor (BD Pharmingen, #556308, San Jose, California).

On removal from the primary antisera, the sections of tissue were washed in TBS then incubated in a biotinylated anti-goat IgG (1:400) for 30 min before being placed in a solution of avidin-biotin peroxidase complex (ABC Kit, Vector labs, Burlingame, CA). Peroxidase chromogen was generated in 0.022% 3,3′-diaminobenzidine (DAB, Aldrich, Milwaukee, WI) and 0.003% hydrogen peroxide in TBS for 6 min. To minimized non-specific attachment of gold particles, the tissue was placed in 0.8% BSA and 0.1% gelatin in phosphate buffered saline (PBS, pH 7.4) before incubation in colloidal ultra-small (0.6 nm) gold particles conjugated to a rabbit anti-mouse antibody (1:50; Amersham Pharmacia Biotech, Piscataway, NJ). Sections were then washed with 0.1 M TBS and incubated in 2% glutaraldehyde. NR1 immunogold labeling was then silver-enhanced (Amersham Pharmacia Biotech, Piscataway, NJ) to increase size and therefore visibility of the gold particles.

Antisera Characterization

CaMKII antibody specificity was evaluated by preincubation with a blocking peptide corresponding to an internal amino-acid sequence of the human CaMKII-α protein (C-PRTAQSEETRVWHR; Abcam, ab126462, Cambridge, MA). Preincubation with the blocking peptide resulted in a loss of labeling in the BLA (Figure 1). The NR1 antibody has been used for immunolabeling in rat and mouse brain (Rodríguez, et al., 1999; Fitzgerald, et al., 2012). Specificity of the NR1 antibody was previously characterized via immunoprecipitation and immunohistochemical means, including electron microscopic studies in the hippocampus and in many other brain regions (Brose et al., 1994; Siegel et al.,

1994; 1995). Western blot analysis of monkey hippocampal homogenates and rat synaptic membranes probed with the NR1 antibody resulted in one major band at ~116kD. HEK 293 cells transfected with cDNA encoding NR1 displayed similar results whereas non-transfected cells probed with the NR1 antibody resulted in no bands (Siegel et al., 1994). Additional dual-labeling controls included processing tissue for dual immunoperoxidase and immunogold-silver labeling with omission of primary antisera, which effectively removed the immunolabeling.

Electron microscopic tissue processing and data analysis

The labeled tissue was post-fixed for one hr in 2% osmium tetroxide, dehydrated through a series of ethanols and propylene oxide, and flat-embedded in Epon 812 resin (Electron Microscopy Sciences, Fort Washington, PA) between two sheets of Aclar plastic. The BLA was then excised from the embedded sections, glued onto hardened plastic blocks and trimmed in preparation for ultrathin sectioning. Light microscopy images of the trimmed blocks were used as a 'map,' which documented the position of labeled elements, regional borders, and tissue landmarks (such as blood vessels). Ultrathin sections (~70 nm) were then cut from the blockface using a diamond knife and an ultramicrotome (Leica, Deerfield, IL). These ultrathin sections were collected on supermesh grids, washed and dried for electron microscopic analysis at 60kV with a Phillips CM10 transmission electron microscope (FEI, Hillsboro, OR). In each thin section, only those portions of the tissue contiguous with the plastic/tissue interface were microscopically examined, thus ensuring quantification of labeling where antibody penetrance was not a limiting factor (Chan et al., 1990). An AMT Advantage HR/HR-B CCD camera (Advantage Microscopy Techniques, Danvers, MA) interfaced with the electron microscope was used to collect digital images at 19,000x in fields containing at least two or more immunogold-labeled profiles with or without immunoperoxidase labeling. The image collection and data analysis was done by an investigator unaware of whether the tissue was derived from group or isolation reared mice.

Electron microscopic images from a total sampled tissue area of 8,147 μm^2 in the isolates and 10,076 μm^2 in the group-reared animals were analyzed using MCID Elite software (v. 6, Imaging Research, Ontario, Canada). CaMKII-immunoperoxidase labeling was recognized by the dark, patchy precipitate, while more punctate electron-dense deposits were defined as immunogold-silver particles. Both types of labeling were predominately seen in profiles having the morphological characteristics of dendrites and dendritic spines that were identified mainly by absence of synaptic vesicles and receipt of synaptic input from vesicle-filled axon terminals (Peters et al., 1991). The number of immunogold-silver particles was analyzed in 1,849 dendritic and 867 spinous profiles, whose perimeter, cross-sectional diameter, and area were determined using the MCID software. From these measurements, we determined the densities rather than simply the ratio of plasmalemmal and cytoplasmic immunogold particles in postsynaptic dendritic profiles to eliminate potential-size-dependent differences that might affect this ratio. Between-group comparisons (isolated-versus group- housed) of the plasmalemmal and cytoplasmic density of NR1-immunogold in CaMKII-labeled profiles were performed using the Student's t-test. This method was also used to determine if these groups significantly differed in the size or number of postsynaptic dendritic profiles that contained NR1-immunogold alone or together with CaMKII immunoreactivity.

Results

ASI-induced Behavioral abnormalities

Acoustic startle testing showed a deficit in PPI in adult mice housed in isolation through the adolescent period of development. Startle was less inhibited when preceded by an 87 dB

prepulse (28.05 ± 1.938 vs 21.27 ± 2.606, $t(43)=2.101$, $p<0.05$) in ASI animals than those reared in groups (Figure 2).

Adult ASI mice also displayed hyperlocomotion when tested in a novel open-field chamber compared to their group-housed littermates ($F(1,38) =26.25$; $p<0.001$). Significant effect of time (as binned in 10 min intervals for the hour session) demonstrated some acclimation to the novel environment time as a factor; $F(1,38) = 8.789$; $p<0.001$; Figure 3).

Subcellular distribution and ASI-induced relocation of NR1 in the BLA

Immunogold-silver particles identifying NR1 were present alone (Figure 4a, 4c, 5c) or together with peroxidase labeling for CaMKII in somatodendritic and axonal profiles in the BLA (Figures 4–5) in all mice, irrespective of rearing conditions. A quantitative analysis of dendritic profiles, which are major targets of glutamatergic terminals, revealed important differences in NR1 density in dendritic spines. The axonal NR1 immunogold distribution was not quantitatively compared in the BLA of mice subject to these different rearing conditions because many of the axonal profiles in this region originate from glutamatergic neurons in other brain regions (LeDoux, 2000).

Almost half (283/584) of the CaMKII-immunoreactive dendritic spines contained NR1-immunogold-silver particles regardless of rearing conditions. Spines were identified by having either an evident post-synaptic density (PSD) or spine apparatus as well as by the absence of mitochondria (Peters et al., 1991). The NR1 labeling in spines was predominately located in the cytoplasm, but also was observed on the extrasynaptic plasmalemmal surface and infrequently in the PSD (Figures 4–5). Quantitative assessment of the density of immunogold-silver particles revealed an isolation rearing-dependent relocation of NR1 from cytoplasmic to plasmalemmal compartments in CaMKII-containing dendritic spines. The cytoplasmic density of NR1 in spines was decreased in isolated compared with group reared animals (4.72±0.517 vs 6.31 ± 0.517 particles per μm^2, $t(281)=1.998$, $p<0.05$). In contrast, the spines from isolates showed a significant increase in plasmalemmal NR1 immunogold-silver density compared with the group reared mice (0.397±0.0779 vs 0.216±0.026 particles per μm, $t(232)=2.829$, $p<0.01$). Total cytoplasmic and plasmalemmal immunogold-silver NR1 density was not significantly different between rearing conditions (8.04±0.662 vs 9.261 ± 0.6443 particles per μm^2, $t(360)=1.32$, $p=0.19$; Figure 6).

Immunogold-silver labeling of NR1 was prevalent in both the plasmalemmal and intracellular compartments of CaMKII-containing dendritic shafts in the BLA pf both isolated (Figure 4) and group-reared (Figure 5). These particles were often located on or near endomembranes and vesicular bodies in both isolated and group-housed animals. Isolation rearing did not alter NR1 densities in the intracellular (2.15±0.172 vs 2.12±0.114 particles per μm^2, $t(654)=0.1727$, $p=0.86$) or plasmalemmal (0.306±0.0157 vs 0.304±0.0130 particles per μm, $t(186)=0.07359$, $p=0.94$) compartments, or collectively in both compartments (2.371±0.1162 vs 2.199±0.1042, $t(1064)=1.10$, $p=0.27$) of the dendritic shafts of BLA principal neurons (Figure 7). Cluster analysis, in which the densities of NR1-labeling was separated based on the area of the dendritic profile (small, medium, large), revealed no significant difference in the NR1 densities regardless of the size of the dendrite (not shown).

Morphometric Analysis of BLA principal neurons

Morphometric analysis showed that adolescent rearing had no significant effect on the number/tissue area, shape or size of dendrites or spines of BLA principle neurons identified by the presence of CaMKII immunolabeling. Similar densities of CaMKII-containing dendrites (2.65±0.910 vs 1.97±0.285; $t(16)=2.12$, $p=0.09$) and dendritic spines (1.50±0.766

vs 0.87594±0.185; t(16)=2.12, p=0.08) were found in isolation and group-housed animals. Morphometry of CaMKII-containing dendrites from isolates or group-reared mice were statistically indistinguishable with regards to the mean area (0.769±0.0173 vs 0.729±0.0227 μm^2, t(359)=1.97, p=0.97); perimeter (0.187±0.00684 vs 0.192±0.0111 μm, t(800)=0.238, p=0.81), length of major axis (1.26±0.0166 vs 1.20±0.0224 μm, t(800)=0.329, p=0.74), or length of minor axis (0.671±0.00718 vs 0.661±0.0105 μm, t(800)=0.275, p=0.78). CaMKII-containing dendritic spines in the BLA of mice reared as isolates or social groups also were statistically indistinguishable with regards to the mean area (3.86±0.0501 vs 3.69±0.0650 μm^2, t(281)=0.90, p=0.37) perimeter (1.82±0.0341 vs 1.83±0.0569 μm, t(281)=0.894, p=0.37), length of major axis (0.603±0.0112 vs 0.610±0.0181 μm, t(281)=1.66, p=0.10), or length of minor axis (0.305±0.00645 vs 0.311±0.0101 μm, t(281)=1.46, p=0.15) (Table 1). In all, analysis revealed no differences between group- and isolation-reared animals in the structural features of principal neurons in the BLA (not shown). There also were no observed differences in the morphology of NR1-containing dendritic spines without detectable CaMKII in terms of area (0.125±0.00482 vs 0.118±0.00346 μm^2, t(987)=1.96, p=0.22) or perimeter (1.50±0.0319 vs 1.44±0.0229 μm, t(988)=1.96, p=0.17).

Discussion

Our results provide ultrastructural evidence for a redistribution of NMDA receptors in dendritic spines of principal neurons in the mature BLA of mice subject to adolescent social isolation, a neurodevelopmental intervention in which animals display behaviors thought to correlate with emotional dysregulation seen in mental health disorders. The finding of a reduction in PPI and hyperlocomotion is consistent with prior studies of ASI mice (Geyer and Moghaddam, 2002). The present demonstration that ASI results in emotional dysregulation and a cytoplasmic to plasmalemmal redistribution of the essential NMDA NR1 subunit in dendritic spines of CaMKII projection neurons of the adult BLA reinforces the dominant effect of adverse developmental experiences on the transport and function of NMDA receptors in the BLA circuitry (Barria and Malinow, 2002; Lau and Zukin, 2007). The abnormal trafficking of NMDA receptors could at least partially underlie the behavioral changes observed when activation of specifically the BLA is disrupted (Adamec, 1991; Stuber et al., 2011).

Adolescent isolation alters NR1 compartmentalization in dendritic spines of BLA projection neurons

The present demonstration that ASI produces a decrease in NMDA NR1 immunogold-silver density in the cytoplasm as well as an increase in the density of these subunits on the plasma membrane of CAMKII-containing dendritic spines of the BLA is consistent with increased surface trafficking and assembly of functional NMDA receptors. This conclusion is strengthened by absence of changes in the total (plasmalemmal and cytoplasmic) density of NR1 immunogold in these spines and by the lack of changes in dendritic spine size, since morphometry as defined by area, perimeter, average diameter and axes, was not affected by rearing conditions. However, this does not exclude the possibility that the observed compartmental redistribution of NR1 in CaMKII-containing dendritic spines of isolation-reared mice is not a reflection of reduced internalization of NMDA receptors.

Many of the extrasynaptic NR1 immunogold particles seen in dendritic spines of principal neurons of the BLA of isolates were distributed within an area that would facilitate rapid stimulus-induced lateral insertion to the PSD (Perez-Otano et al., 2004; Lau and Zukin, 2007;. However, NR1 immunogold labeling in postsynaptic densities was notably more sparse than on extrasynaptic plasma membranes of dendritic spines, a distribution effect that may be at least partially driven by limited antibody penetration in pre-embedding immunocytochemistry (Milner et al., 2011). The use of this method enables the detection of

extrasynaptic receptors that are often not identifiable after plastic embedding (Adams et al., 2002). Certain extrasynaptic receptors will be laterally mobilized to the PSD, but many others are locally activated by extracellular glutamate that diffuses from the synapse or is released by neighboring glia (Barria and Malinow, 2005). One important aspect of these extrasynaptic NMDA receptors is that they more often contain NR2B subunits, which have different receptor kinetics than those that contain NR2A subunits (Barria and Malinow, 2005; Carpenter-Hyland and Chandler, 2007). During maturation, NMDA-dependent plasticity is altered due to a developmental shift in receptor composition, where the ratio between NR2A-containing and NR2B-containing receptors dramatically increases (Williams et al., 1993; Monyer et al., 1994;). Since insertion of NR2A-containing receptors is activity dependent (Barria and Malinow, 2002), neuronal activity evoked by social play during adolescence may be important for proper maturation of NMDA receptor populations (Spear, 2000). Even though the precise timeline of the switch in NMDA subunit composition is still unknown, disruptions to this ontogenetic phenomenon may contribute to at least some of the maladaptive behavioral syndrome produced by adolescent social isolation.

The increased density of mainly extrasynaptic plasmalemmal NR1 immunogold particles in CaMKII-containing dendritic spines of ASI reared rodents might also make these spines more vulnerable to destruction by synaptic activity (Hardingham and Bading, 2003). However, this seems unlikely because the isolated and group reared mice did not differ in number of CaMKII-containing dendritic spines per unit area of BLA tissue. The lack of ASI-induced changes in spine density in the BLA suggests that this psychosocial stress differs from other types of chronic stress, which have been shown to produce a long-lasting increase in BLA spine density correlated with enhanced anxiety-like behaviors (Vyas et al., 2006). These authors also found an increase in the dendritic arborization of principal neurons in the BLA after prolonged stress, which is comparable to that seen in the adult BLA of ASI rats (Wang et al., 2012). However, the lack of change in the mean number or size of dendritic profiles in the present study suggests that this does not occur in C57/BL6 mice. This potential species differences is consistent with the less robust effect of social isolation on PPI deficits in mice compared with rats.

The age-dependent differences in the effects of stress on the dendritic cytoarchitecture in the BLA is consistent with the hypothesis that the presently observed NMDA receptor redistribution in dendrites and dendritic spines of the BLA results from the psychosocial stress of adolescent isolation. In contrast with the long lasting effects of ASI, the acute stress of acoustic startle begin and end rapidly (Davis et al., 2010) suggesting a minimal contribution to NMDA receptor trafficking after a one week delay between PPI testing and processing of brain tissue for electron microscopy in the present study.

Conclusion

The results of this study indicate that ASI produces a selective redistribution of NR1 subunits in dendritic spines of projection neurons in the BLA, where the prominent extrasynaptic location of these subunits is consistent with an increased population of NR1/NR2B containing NMDA receptors. This suggests that ASI-induced changes in the subcellular location and/or composition of NMDA receptors in principal neurons of the BLA may diminish baseline synaptic transmission and network activity that is crucial for sensorimotor gating and other behaviors that are dysfunctional in multiple psychiatric disorders (Geyer and Moghaddam, 2002; Spear, 2011). Additional studies are necessary to uncover the potentially crucial contribution of the developmentally regulated NR2B receptor subunits in this process.

Acknowledgments

The authors gratefully acknowledge the intellectual input on adolescent isolation from Dr. Megan Fitzgerald and funding provided by the National Institutes of Health (MH40342 and DA004600 to VMP).

Abbreviations

ASI	adolescent social isolation
BLA	basolateral amygdala
PSD	post-synaptic density
CaMKII	calcium calmodulin dependent protein kinase II
PPI	prepulse inhibition

Reference List

Adamec RE. Individual differences in temporal lobe sensory processing of threatening stimuli in the cat. Physiology & Behavior. 1991; 49(3):455–464. [PubMed: 1648240]

Adams MM, Fink SE, Shah RA, Janssen WGM, Hayashi S, Milner TA, McEwen BS, Morrison JH. Estrogen and aging affect the subcellular distribution of estrogen receptor-alpha in the hippocampus of female rats. J Neurosc. 2002; 22:3608–3614.

Adell A, Jiménez-Sánchez L, López-Gil X, Romón T. Is the acute NMDA receptor hypofunction a valid model of schizophrenia? Schizophrenia Bulletin. 2012; 38:9–14. [PubMed: 21965469]

Bakshi VP, Geyer MA. Multiple limbic regions mediate the disruption of prepulse inhibition produced in rats by the noncompetitive NMDA antagonist dizocilpine. J Neurosci. 1998; 18:8394–8401. [PubMed: 9763482]

Barria A, Malinow R. Subunit-specific NMDA receptor trafficking to synapses. Neuron. 2002; 35:345–353. [PubMed: 12160751]

Barria A, Malinow R. NMDA receptor subunit composition controls synaptic plasticity by regulating binding to CaMKII. Neuron. 2005; 48:289–301. [PubMed: 16242409]

Bechara A, Damasio H, Damasio AR, Lee GP. Different contributions of the human amygdala and ventromedial prefrontal cortex to decision-making. J Neurosci. 1999; 19:5473–5481. [PubMed: 10377356]

Belforte JE, Zsiros V, Sklar ER, Jiang Z, Yu G, Li Y, Quinlan EM, Nakazawa K. Postnatal NMDA receptor ablation in corticolimbic interneurons confers schizophrenia-likephenotypes. Nat Neurosci. 2009; 13:76–83. [PubMed: 19915563]

Benes FM. Amygdalocortical Circuitry in Schizophrenia: From Circuits to Molecules. Neuropsychopharmacology. 2009; 35:239–257. [PubMed: 19727065]

Braff DL, Geyer MA. Sensorimotor gating and schizophrenia. Human and animal model studies. Arch Gen Psychiatry. 1990; 47:181–188. [PubMed: 2405807]

Brose N, Huntley GW, Stern-Bach Y, Sharma G, Morrison JH, Heinemann SF. Differential assembly of coexpressed glutamate receptor subunits in neurons of rat cerebral cortex. J Biol Chem. 1994; 269:16780–16784. [PubMed: 8207001]

Carpenter-Hyland EP, Chandler LJ. Adaptive plasticity of NMDA receptors and dendritic spines: implications for enhanced vulnerability of the adolescent brain to alcohol addiction. Pharmacol Biochem Behav. 2007; 86:200–208. [PubMed: 17291572]

Chan J, Aoki C, Pickel VM. Optimization of differential immunogold-silver and peroxidase labeling with maintenance of ultrastructure in brain sections before plastic embedding. J Neurosci Methods. 1990; 33:113–127. [PubMed: 1977960]

Cunningham MG, Bhattacharyya S, Benes FM. Amygdalo-cortical sprouting continues into early adulthood: implications for the development of normal and abnormal function during adolescence. J Comp Neurol. 2002; 453:116–130. [PubMed: 12373778]

Davis M, Walker DL, Miles L, Grillon C. Phasic vs sustained fear in rats and humans: role of the extended amygdala in fear vs anxiety. Neuropsychopharmacology. 2010; 35:105–135. [PubMed: 19693004]

Einon DF, Morgan MJ. A critical period for social isolation in the rat. Dev Psychobiol. 1977; 10:123–132. [PubMed: 838157]

Fendt M. Injections of the NMDA receptor antagonist aminophosphonopentanoic acid into the lateral nucleus of the amygdala block the expression of fear-potentiated startle and freezing. J Neurosci. 2001; 21:4111–4115. [PubMed: 11356899]

Fitzgerald ML, Chan J, Mackie K, Lupica CR, Pickel VM. Altered dendritic distribution of dopamine D2 receptors and reduction in mitochondrial number in parvalbumin-containing interneurons in the medial prefrontal cortex of cannabinoid-1 (CB1) receptor knockout mice. J Comp Neurol. 2012; 520:4013–4031. [PubMed: 22592925]

Geyer, MA.; Moghaddam, B. Animal models relevant to schizophrenia disorders. 2002. p. 1-14.

Hara Y, Pickel VM. Overlapping intracellular and differential synaptic distributions of dopamine D1 and glutamate N-methyl-D-aspartate receptors in rat nucleus accumbens. J Comp Neurol. 2005; 492:442–455. [PubMed: 16228995]

Hardingham GE, Bading H. The Yin and Yang of NMDA receptor signalling. Trends in Neurosci. 2003; 26:81–89.

Insel T, Cuthbert B, Garvey M, Heinssen R, Pine DS, Quinn K, Sanislow C, Wang P. Research domain criteria (RDoC): toward a new classification framework for research on mental disorders. Am J Psychiatry. 2010; 167:748–751. [PubMed: 20595427]

Jacobs SA, Tsien JZ. genetic overexpression of NR2B subunit enhances social recognition memory for different strains and species. PLoS One. 2012; 7:e36387. [PubMed: 22558458]

Kristiansen LV, Bakir B, Haroutunian V, Meador-Woodruff JH. Expression of the NR2BNMDA receptor trafficking complex in prefrontal cortex from a group of elderly patients with schizophrenia. Schizophrenia Research. 2010; 119:198–209. [PubMed: 20347576]

Lau CG, Zukin RS. NMDA receptor trafficking in synaptic plasticity and neuropsychiatric disorders. Nat Rev Neurosci. 2007; 8:413–426. [PubMed: 17514195]

LeDoux JE. Emotion circuits in the brain. Annu Rev Neurosci. 2000; 23:155–184. [PubMed: 10845062]

Levine JB, Youngs RM, MacDonald ML, Chu M, Leeder AD, Berthiaume F, Konradi C. Isolation rearing and hyperlocomotion are associated with reduced immediate early gene expression levels in the medial prefrontal cortex. Neuroscience. 2007; 145:42–55. [PubMed: 17239545]

Lukkes JL. Consequences of post-weaning social isolation on anxiety behavior and related neural circuits in rodents. Front Behav Neurosci. 2009; 3:18. [PubMed: 19738931]

Lukkes JL, Burke AR, Zelin NS, Hale MW, Lowry CA. Post-weaning social isolation attenuates c-Fos expression in GABAergic interneurons in the basolateral amygdala of adult female rats. Physiol Behav. 2012; 107:719–25. [PubMed: 22583860]

McDonald AJ. Projection neurons of the basolateral amygdala: a correlative Golgi and retrograde tract tracing study. Brain Res Bull. 1992; 28:179–185. [PubMed: 1375860]

Milner, TA.; Waters, EM.; Robinson, DC.; Pierce, JP. Methods in Molecular Biology. Totowa, NJ: Humana Press; 2011. Degenerating Processes Identified by Electron Microscopic Immunocytochemical Methods; p. 23-59.Methods in Molecular Biology

Monyer H, Burnashev N, Laurie DJ, Sakmann B, Seeburg PH. Developmental and regional expression in the rat brain and functional properties of four NMDA receptors. Neuron. 1994; 12:529–540. [PubMed: 7512349]

Paxinos, G.; Franklin, KBJ. The Mouse Brain in Stereotaxic Coordinates: Compact Second Edition, Second Edition. 2. Academic Press; 2003.

Perez-Otano I, Ehlers MD. Learning from NMDA Receptor Trafficking: Clues to the development and maturation of glutamatergic synapses. Neurosignals. 2004; 13:175–189. [PubMed: 15148446]

Perez-Otano I, Ehlers MD. Homeostatic plasticity and NMDA receptor trafficking. Trends Neurosci. 2005; 28:229–238. [PubMed: 15866197]

Peters, A.; Palay, S.; Webster, H. The Fine Structure of the Nervous System. New York: Oxford University Press; 1991.

Pietropaolo S, Singer P, Feldon J, Yee BK. The postweaning social isolation in C57BL/6 mice: preferential vulnerability in the male sex. Psychopharmacology. 2008; 197:613–628. [PubMed: 18317735]

Radley JJ, Farb CR, He Y, Janssen WGM, Rodrigues SM, Johnson LR, Hof PR, LeDoux JE, Morrison JH. Distribution of NMDA and AMPA receptor subunits at thalamoamygdaloid dendritic spines. Brain Research. 2007; 1134:87–94. [PubMed: 17207780]

Rodríguez JJ, Garcia DR, Pickel VM. Subcellular distribution of 5-hydroxytryptamine2A and N-methyl-D-aspartate receptors within single neurons in rat motor and limbic striatum. J Comp Neurol. 1999; 413:219–231. [PubMed: 10524335]

Rubio MD, Wood K, Haroutunian V, Meador-Woodruff JH. Dysfunction of the ubiquitin proteasome and ubiquitin-like systems in schizophrenia. Neuropsychopharm. 2013; 38:1910–20.

Siegel SJ, Brose N, Janssen WG, Gasic GP, Jahn R, Heinemann SF, Morrison JH. Regional, cellular, and ultrastructural distribution of N-methyl-D-aspartate receptor subunit 1 in monkey hippocampus. Proc Natl Acad Sci USA. 1994; 91:564–568. [PubMed: 8290563]

Siegel SJ, Janssen WG, Tullai JW, Rogers SW, Moran T, Heinemann SF, Morrison JH. Distribution of the excitatory amino acid receptor subunits GluR2(4) in monkey hippocampus and colocalization with subunits GluR5–7 and NMDAR1. J Neurosci. 1995; 15:2707–2719. [PubMed: 7722624]

Spear LP. The adolescent brain and age-related behavioral manifestations. Neurosci Biobehav Rev. 2000; 24:417–463. [PubMed: 10817843]

Spear LP. Rewards, aversions and affect in adolescence: emerging convergences across laboratory animal and human data. Dev Cogn Neurosci. 2011; 1:392–400. [PubMed: 21918675]

Stevenson CW, Gratton A. Basolateral amygdala dopamine receptor antagonism modulates initial reactivity to but not habituation of the acoustic startle response. Behav Brain Res. 2004; 153:383–387. [PubMed: 15265633]

Stuber GD, Sparta DR, Stamatakis AM, van Leeuwen WA, Hardjoprajitno JE, Cho S, Tye KM, Kempadoo KA, Zhang F, Deisseroth K, Bonci A. Excitatory transmission from the amygdala to nucleus accumbens facilitates reward seeking. Nature. 2011; 475:377–380. [PubMed: 21716290]

Tye KM, Prakash R, Kim S-Y, Fenno LE, Grosenick L, Zarabi H, Thompson KR, Gradinaru V, Ramakrishnan C, Deisseroth K. Amygdala circuitry mediating reversible and bidirectional control of anxiety. Nature. 2011; 471:358–362. [PubMed: 21389985]

Vyas A, Jadhav S, Chattarji S. Prolonged behavioral stress enhances synaptic connectivity in the basolateral amygdala. Neuroscience. 2006; 143:387–393. [PubMed: 16962717]

Wang Y-C, Ho U-C, Ko M-C, Liao C-C, Lee L-J. Differential neuronal changes in medial prefrontal cortex, basolateral amygdala and nucleus accumbens after postweaning social isolation. Brain Struct Funct. 2012; 217:337–351. [PubMed: 22002740]

Wenthold RJ, Prybylowski K, Standley S, Sans N, Petralia RS. Trafficking of NMDA Receptors. Annu Rev Pharmacol Toxicol. 2003; 43:335–358. [PubMed: 12540744]

Williams K, Russell SL, Shen YM, Molinoff PB. Developmental switch in the expression of NMDA receptors occurs *in vivo* and *in vitro*. Neuron. 1993; 10:267–278. [PubMed: 8439412]

Highlights

- Adolescent social isolation (ASI) produces maladaptive adult behaviors.
- The affected behaviors are principally those that require emotional processing.
- ASI produces an increase in NMDA receptors in spines of amygdala output neurons.
- Potentiation of these output neurons may contribute to ASI behavioral abnormality.

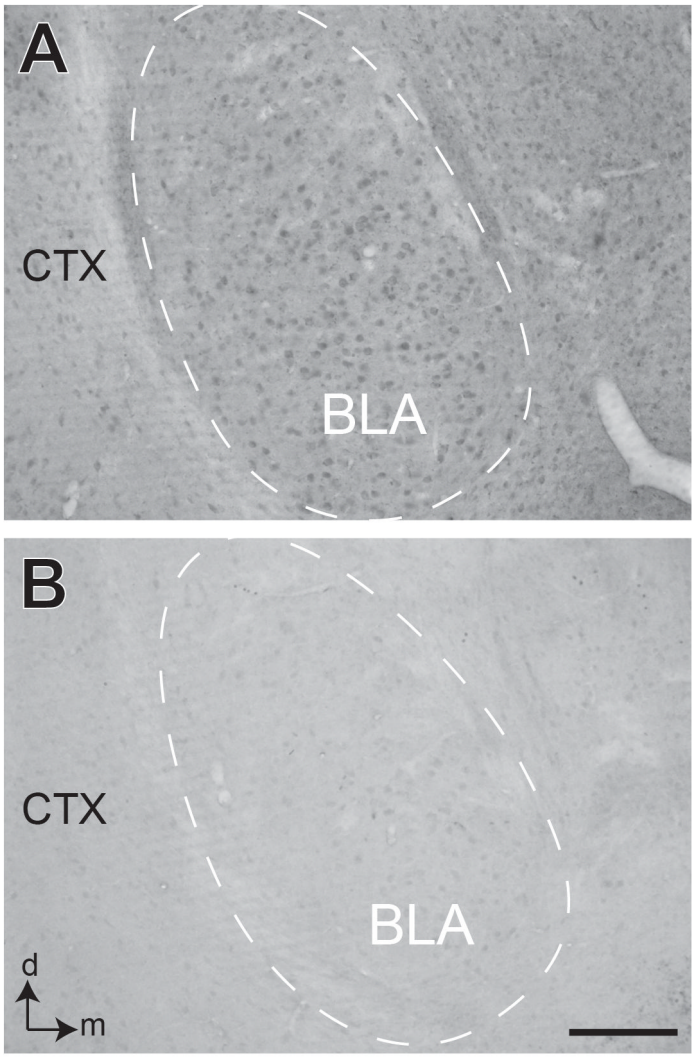

Figure 1. Peptide blocking of CaMKII

Light microscopic images showing coronal sections of basolateral amygdala (BLA) (dashed area) processed for immunoperoxidase labeling of CaMKII-α antibody without (A) or with preincubation in a blocking peptide (B). CTX= piriform cortex; d and m = dorsal and medial orientation. Scale bar = 100 μm.

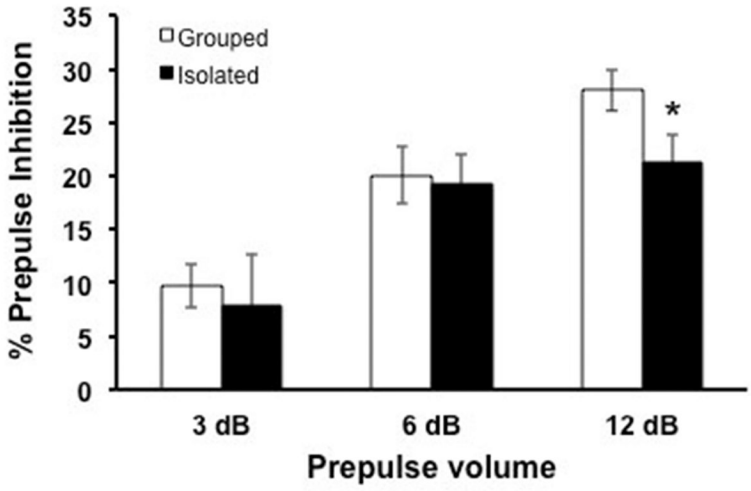

Figure 2. Deficit in PPI after isolation rearing

Percent prepulse inhibition in isolation-reared (n=17) is significantly less than in group-housed (n=23) mice. Animals were tested for startle response when a prepulse (3, 6, or 12 dB above 75 dB background noise) stimulus preceded a startling acoustic stimulus (120dB). Student's t test, *, $p<0.05$.

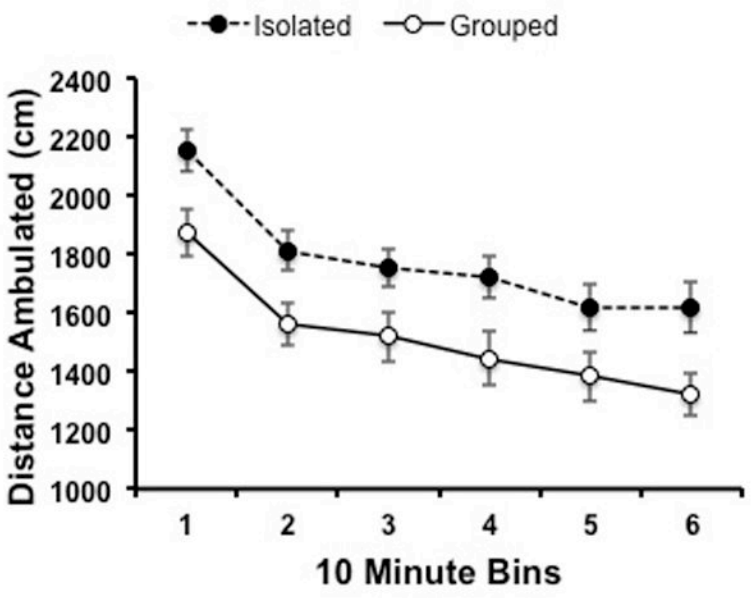

Figure 3. Locomotor response to novel environment in group-housed and isolated animals

Exploratory behavior of group-housed (n=23) and isolated (n=17) animals were assessed for one hour (binned in ten minute intervals) in an open field test. Distance ambulated demonstrated an interaction with rearing conditions as well as time across the behavioral session (2-way ANOVA).

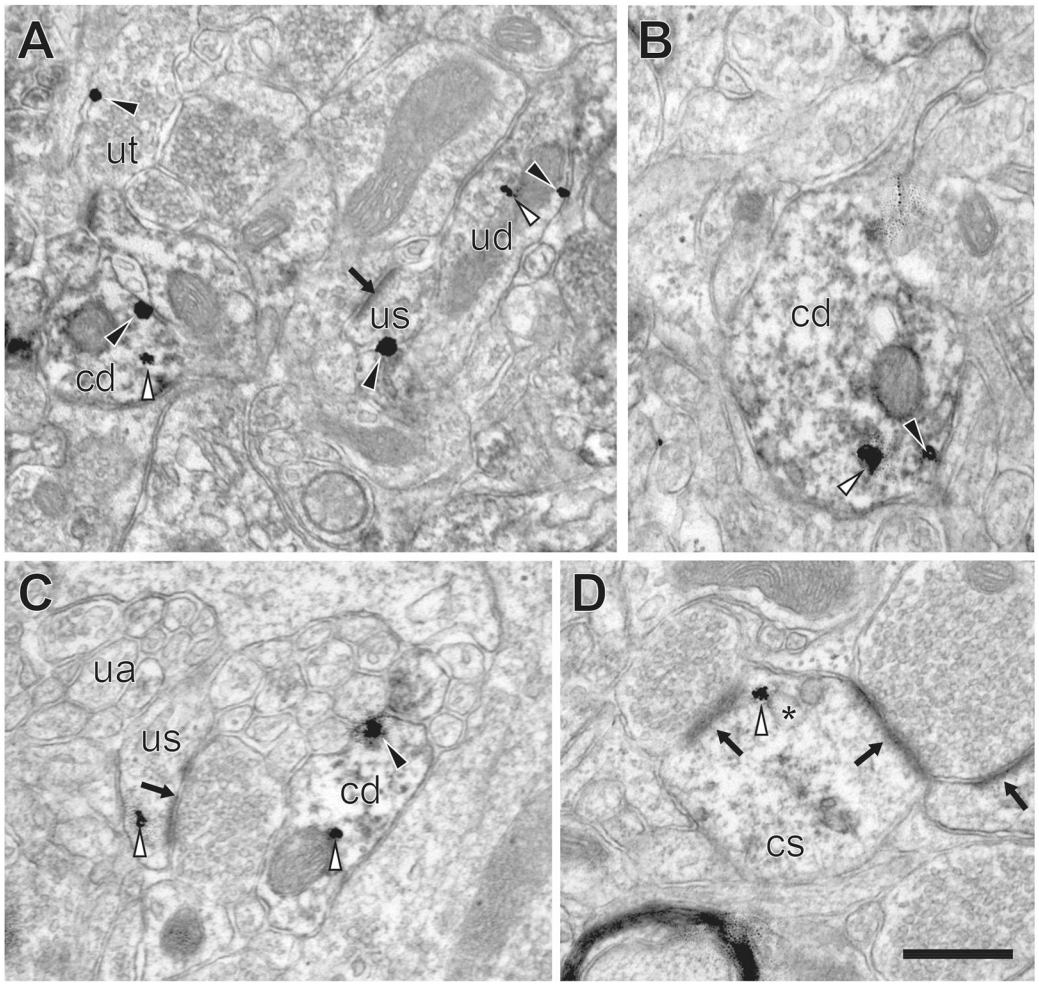

Figure 4. NR1 in basolateral amygdala of group-housed mice

A–C. Immunogold-silver NR1 particles in CaMKII-labeled dendrites (cd) as well as in unlabeled spines (us), dendrites (ud) and terminals (ut). NR1 particles are present both intracellularly (white arrowheads) and on the plasmallemma (black arrowheads). Post-synaptic densities (black arrow) identify asymmetric synapses. A. CaMKII-labeled and unlabeled dendrites as well as non-CaMKII-labeled dendritic spine and terminal containing immunogold-silver particles. B. CaMKII-containing dendrite containing an immunogold-silver particle in the cytoplasm and the plasma membrane. C. Unlabeled axons (ua) are also seen in the neuropil near the dual labeled dendrite. D. NR1 immunogold-silver particles are distributed in the intracellular compartment of CaMKII-labeled spines (cs), often associated with endosomal membranes (*). Scale bar = 0.5 μm.

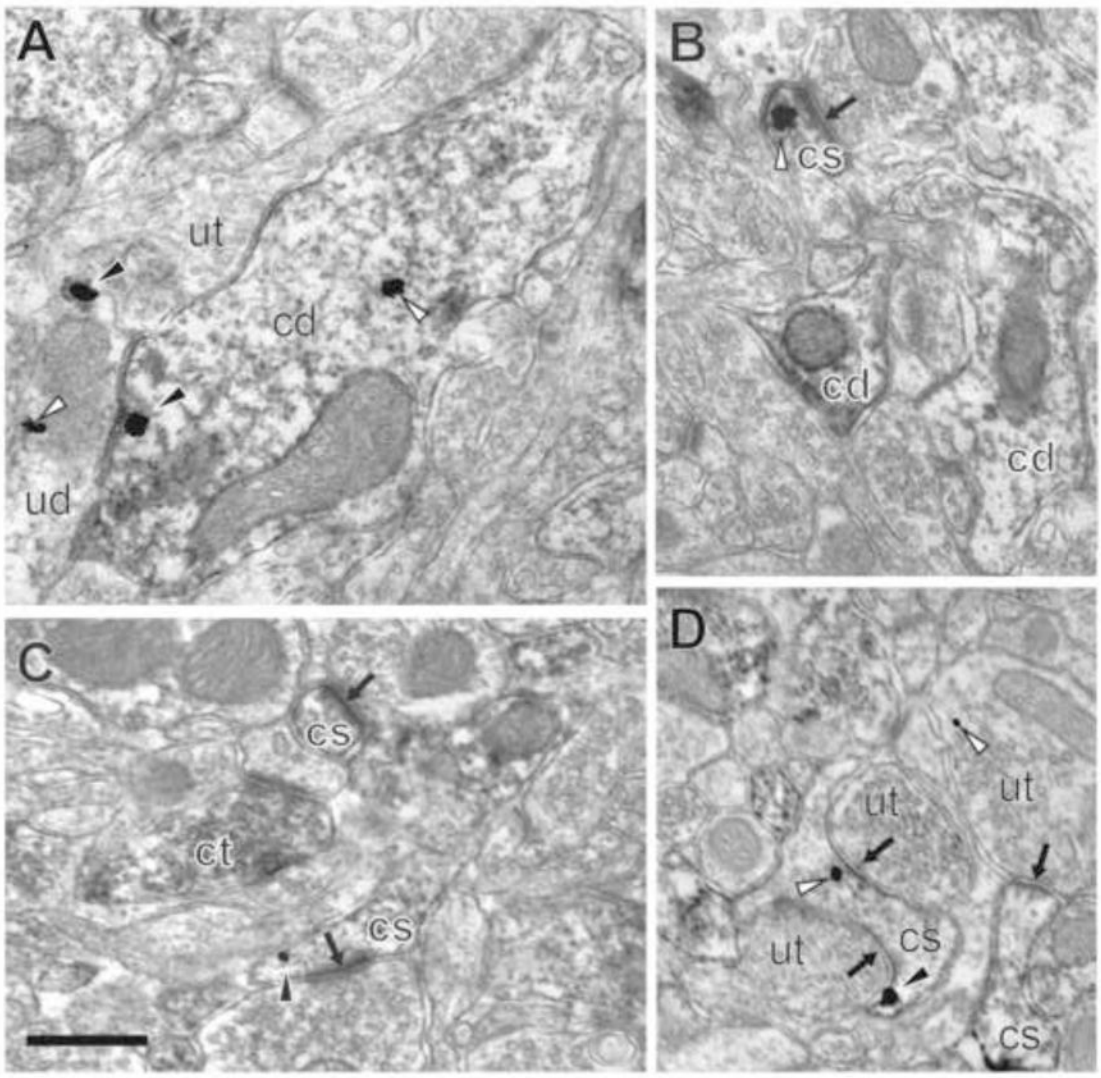

Figure 5. NR1 in basolateral amygdala of socially-isolated mice

A–D. NR1 in the intracellular compartment (white arrowhead) and on the plasma membrane (black arrowhead) of CaMKII-labeled dendrites (cd) and dendritic spines (cs) containing postsynaptic densities (black arrow). A. CaMKII-containing dendrite abutting an unlabeled terminal (ut) and unlabeled dendrite (ud) in the basolateral amygdala of a socially-isolated mouse. B. CaMKII-containing dendrites and a dendritic spine containing a cytoplasmic immunogold-silver particle. C. CaMKII-labeled terminal (ct) near CaMKII-labeled spines. D. CaMKII-labeled spine with perisynaptic NR1 (black arowhead) contacted by unlabeled terminals. Scale bar = 0.5 μm.

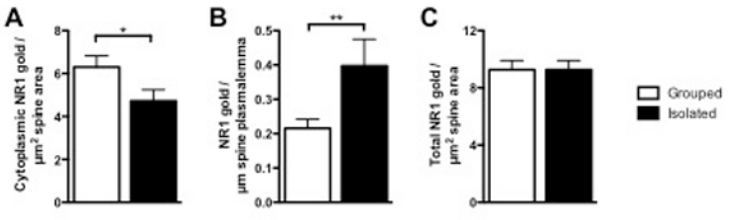

Figure 6. Distribution of NR1 in dendritic spines of CaMKII-containing neurons in the basolateral amygdala in group and isolated mice

Bar graphs showing NR1 immunogold-silver density in the cytoplasm (A), on the plasmalemma (B), and total (cytoplasmic and plasmalemmal) (C) of CaMKII-labeled dendritic spines of adult mice reared in groups or isolation. Student's t test, *, $p<0.05$; **, $p<0.01$; n=4–5.

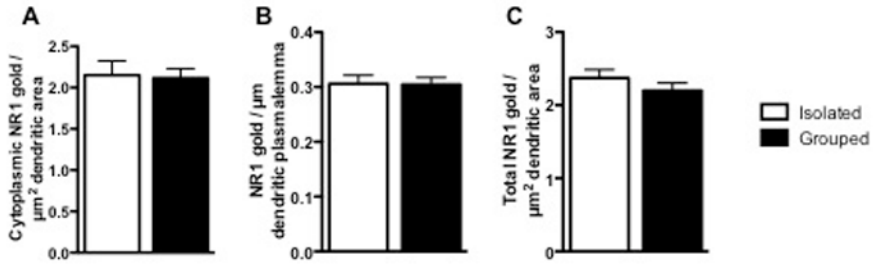

Figure 7. Distribution of NR1 in dendrities of CaMKII-containing neurons in the basolateral amygdala in group and isolated mice

Bar graphs showing NR1 immunogold-silver density in the cytoplasm (A), on the plasmalemma (B), and total (cytoplasmic and plasmalemmal) (C) of CaMKII-labeled dendrites of adult mice reared in groups or isolation. $p>0.05$; $n=4–5$.

Table 1

Morphometric measurements of CaMKII-containing profiles

	Grouped	**Isolated**
Sampled Area (square micron)	10,076 (5 mice)	8147 (4 mice)
Mean Area of dendrites	0.769 ± 0.0173	0.729 ± 0.0227
Mean perimeter of dendrites	0.187 ± 0.00684	0.192 ± 0.0111
Mean area of spines	3.86 ± 0.0501	3.69 ± 0.0650
Mean perimeter of spines	1.82 ± 0.0341	1.83 ± 0.0569
Mean number of dendrites/sq-micron	2.653 ± 0.301	1.97 ± 0.189
Mean number of spines/sq-micron	1.50 ± 0.277	0.876 ± 0.152
Mean major axis dendrites	1.26 ± 0.0166	1.20 ± 0.0224
Mean Minor axis dendrites	0.671 ± 0.00718	0.661 ± 0.0105
Mean major axis spines	0.603 ± 0.0112	0.610 ± 0.0181
Mean Minor axis spines	0.305 ± 0.00645	0.311 ± 0.0101